WORLD JOURNAL OF PHARMACEUTICAL RESEARCH
SJIF Impact Factor 6.805
Volume 5, Issue 6, 486-508. Review Article ISSN 2277– 7105

SYNTHESIS, CHARACTERISATION AND INTERACTION STUDY OF COBALT (III) EDTA AZIDO COMPLEX WITH BSA AND DNA

V.Violet Dhayabaran, M.Malathi, T.Daniel Prakash, V. Kalaiselvi

PG and Research Department of Chemistry, Bishop Heber College, Thiruchirappalli-620017, Tamil Nadu, India.

Article Received on
14 April 2016,
Revised on 04 May 2016,
Accepted on 24 May 2016
DOI: 10.20959/wjpr20166-6267

***Corresponding Author**
Violet Dhayabaran V.
PG and Research Department of Chemistry, Bishop Heber College, Thiruchirappalli-620017, Tamil Nadu, India.

ABSTRACT

Complex has been synthesized by simple chemical method and characterized using Infrared spectral analysis, UV-Visible spectral analysis and Cyclic voltammetry. The interaction between $[Co(HEDTA)N_3]^-$ with BSA and CT-DNA has been studied by UV–visible and Fluorescence spectral analysis. The results presented clearly indicates that the $[Co(HEDTA)N_3]^-$ complex enhances the absorption of BSA and DNA through complex formation. Binding studies of $[Co(HEDTA)N_3]^-$ complex has been investigated with the protein BSA and CT-DNA by UV-Visible spectrometry measurements and the apparent binding constants were determined. Experimental data reveals that the emission profiles of EB in the absence and presence of CT-DNA. EB does not emit fluorescence, but its emission intensity in the presence of DNA is greatly enhanced, due to its not strong intercalation between the adjacent DNA base pairs. Binding studies of $[Co(HEDTA)N_3]^-$ complex has been investigated with the protein BSA and CT-DNA by fluorescence spectral measurement. The binding constant were determined.

KEYWORDS: Cobalt, Azido, DNA, BSA.

INTRODUCTION

Transition metals are a growing area of interest due to their important role in biological processes, electrochemistry, and pharmaceutical synthesis. Also, they are known to possess interesting antimicrobial and antitumour properties. There is growing awareness associated with electrochemical, magnetic and spectroscopic studies of metal complexes due to their biological interest. Upon photoexcitation, these metals can radiate the excited energy by

releasing electrons (photochemically or photophysically), losing ligands and transferring energy (electrons) to nearby species. Photoactivated chemotherapy for d-block metals, such as Ti, V, Cr, Mn, Re, Fe, Ru, Os, Co, Rh, Ir, Au, Pt and Cu, has potential for greater exploration. The photophysics of Ti, V, Fe, Cu, Rh, Pt and Au have been well studied and demonstrated anticancer activity.[3]

Transition metals can be easily excited with visible and UV light, leading to various electronic and vibrational states where orbitals may possess mixed metal/ligand character depending on the class of the metal-ligand bond. Once electrons reach the photoexcited state, several possible photophysical phenomena occur to achieve the ground state electronic structure (intersystem crossing (ISC), internal conversion (IC), vibrational relaxation and salvation dynamics). The lifetime of this metal ion electronic transition is short (50 ns–1 μs) compared to organic compounds, and the quantum yield is quite high for this photo transition. Transition metal complexes having d^3 and d^6 electronic configurations show remarkable photophysical properties.

There are different types of electronic transitions: metal-metal (d-d), ligand field (LF), charge transfer (CT) and ligand centered (LC). Metalcenteredtransitions are mainly orbital forbidden and occasionally spin forbidden, resulting in weak absorption intensities. Metal-centered transitions mostly reside in the antibondingorbitals; thus, photochemical lability favors the release of the ligand (Bioactive NO, CO) and ligand substitution. Charge transfer complexes are defined as involving metal-to-ligand (MLCT), metal-to-solvent (TS) or ligand-to-metal (LMCT) transitions and have intense molar absorptivity. They can trigger redox reactions resulting in free radicals capable of DNA damage under physiological conditions. Photoexcited states of metal complexes such as triplet states de-energize by transferring energy to the ground state triplet oxygen, generating highly reactive singlet oxygen. The energy of the triplet excited state metal complex must be >−94 kJmol−1 in order for this photophysical phenomenon to occur. The excited singlet oxygen has the potential to damage DNA, modify the protein, promote lipid peroxidation and destroy the tumor microenvironment. This process is known as photodynamic therapy (PDT).Cu complexes, havebeen reported to cleave DNA in a photo dependent manner(λ_{irr}=700–755 nm, NIR) and without direct irradiation. With the proposed mechanisms for the DNA damage, inthe presence of O_2, a hydroxyl radical and singlet oxygenare generated, and under hypoxic conditions a sulfuranionic radical is produced.

2. Experimental methods

2.1 Chemicals

Chemicals like $CoCl_2$, Sodium azide, Bromine, H_2O_2, EDTA, BSA and CT- DNA were purchased from Loba chemicals and used without further purification. All the experimental solutions were prepared using double distilled water.

2.2 Synthesis of Complex

The complex was synthesis by chemical method. In briefly, Sodium hydroxide (1.78g) was dissolved in water then hot solution of EDTA (6.8g) was added. A solution of cobalt (II) chloride (6g) in water was added to the mixture in small quantities at a time with constant stirring and then solid sodium azide (6g) was added in a small portion with continued vigorous stirring. Hydrogen peroxide(10ml) solution of known concentration was added in drops and the process of addition was continued for a period of about three hours , temperature and pH of the reaction mixture below 5˚C and around for respectively. Color change from pink to red. The process of stirring was continued for a further period of about two hours. The reaction mixture was then transferred to a beaker containing dry acetone and this caused separation of bluish violet colored solid.

The crude product, thus obtained was dissolved in a minimum quantity of water and the solution was then treated with dry acetone. The process of purification was repeated till pure violet colored crystals of the complex. Separated and these were dried by keeping the crystals in a vacuum desiccator.

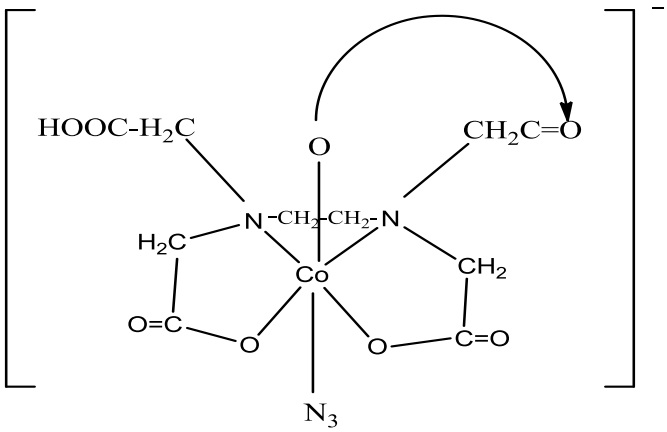

Fig.1 Structure of Azido complex

2 Characterization of the complex

2.1 UV-Visible Absorption spectra

The UV-Visible absorption spectra of the complex $[Co(HEDTA)N_3]^-$ Summarized and shown in Table.1. It found that the values obtained are good agreement with the reported value.

2.2. a. Ligand- field Bands

The electronic configuration of the ground state of cobalt (III) ion, in octahedral symmetry, is t^6_{2g} which gives rise to the term $^1A_{1g}$. The configuration, for one electron excitation, is t^5_{2g}, e_g^1. This excited configuration gives rise to four states, viz., two singlet and two triplets, and these are $^1T_{1g}$, $^1T_{2g}$, $^3T_{1g}$. The energy level diagram for the ligand-field excited states of an octahedral cobalt(III) complex is shown in the following figure.6.

The bands with low intensity are called ligand-field bands. A complex, containing two or more mixed ligands, shows two ligand-fields bands, provided the two ligand are well separated in the spectro chemical series. However, Lever has stated that if that ligand were not well separated, only a band shift or broadening of band would be observed.

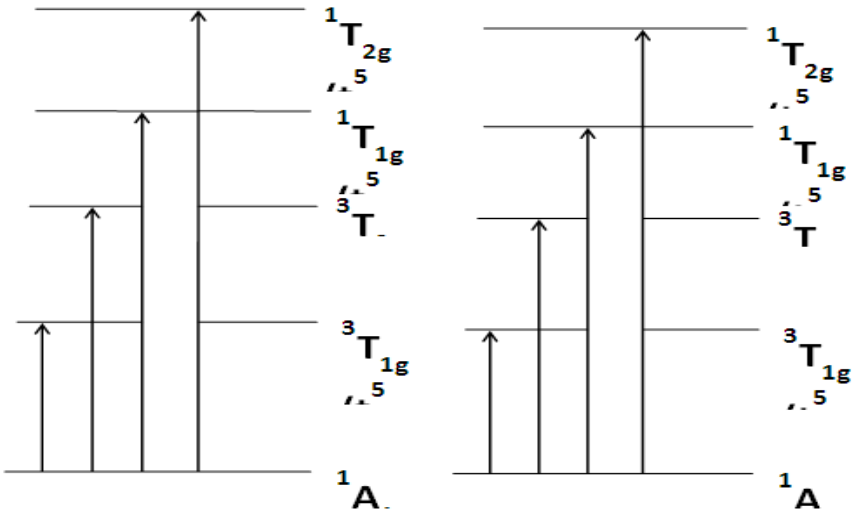

Fig. 6 Energy Level Diagram for the Ligand-field States of Octahedral Cobalt (III) Complexes

Hence, a typical ultraviolet-visible absorption spectra of cobalt (III) complexes are expected to show two typical ligand-field bands in the visible region or in the near ultraviolet region. For instance, the spectrum of $[Co(NH_3)_6]^{3+}$ ion shows two bands at 472 and 380 nm with ϵ values of 55 and 49 dm^3 mol^{-1} cm^{-1} respectively and these bands correspond to ligand-field transitions. The spectrum of $[Co(HEDTA)N_3]^-$ ion shows two ligand-field bands at 380 and

535 nm with ϵ values of 14 and 270 dm^3 mol^{-1} cm^{-1} respectively. The other ligand-field band was observed as a shoulder, hidden in the tail of the more intense charge-transfer band.

b. Charge transfer bands

An analysis of UV absorption data reveals the presence of two charge transfer band one at 225 and another at 315 nm it is also included agreement with reported values and represented in table.1.

UV-Visible spectrum of $[Co(HEDTA)N_3]^-$ is shown in Fig.8 and the values are represented in table.1.

Table. 1 Ligand-field and Charge transfer Band.

Name of the complex	Ligand-Field Band		Charge Transfer Band	
	λ_{max}(nm)	Ε, dm^3 mol^{-1} cm^{-1}	λ_{max}(nm)	Ε, dm^3 mol^{-1} cm^{-1}
$[Co(HEDTA)N_3]^-$	560	225	254	11,815
		315		6,805
$[Co(HEDTA)Br]^-$	592	235	252	15,840
		278		1 6,670

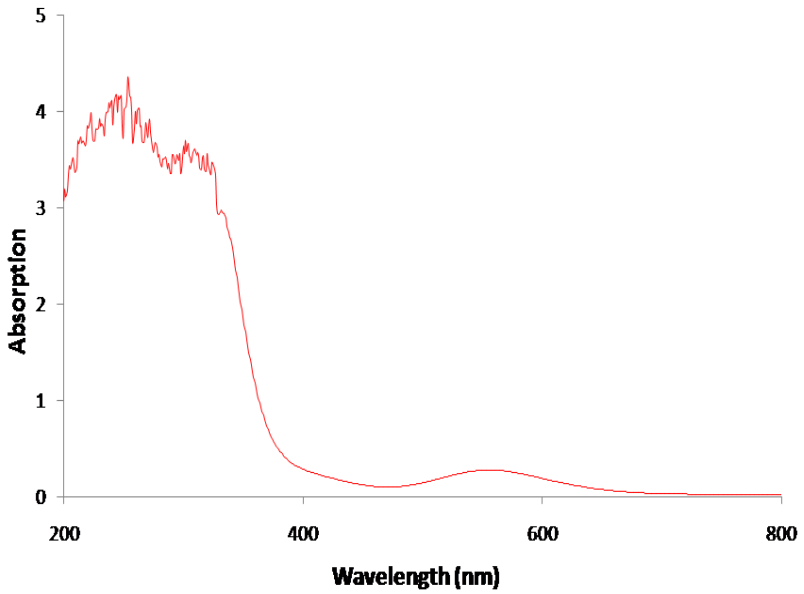

Fig. 7 UV-Visible spectra of $[Co(HEDTA)N_3]^-$ complex

2.3 Infra-red Spectrometry

In the infra-red spectra of azide complex ion is recorded and shown in fig.8 the frequency corresponding to Azide, co-ordinated, ionic carboxylate ion are given in table.

Table. 2 Infra-red spectra of azide complex

Name of the complex	Azide (cm^{-1})	$V_{co\text{-}ordinated}$(cm^{-1})	$V_{ion\text{-}coo^-}$ (cm^{-1})
$[Co(HEDTA)N_3]^-$	2053	1640	1370

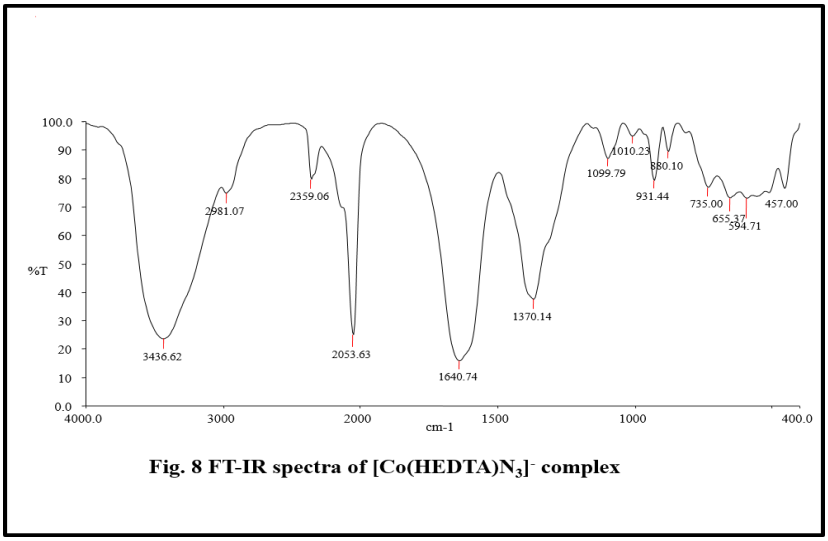

Fig. 8 FT-IR spectra of $[Co(HEDTA)N_3]^-$ complex

3.4 Cyclic Voltammetry

Cyclic Voltammetry of $[Co(HEDTA)N_3]^-$ complex were synthesized. Doubly distilled water was used throughout. Phosphate buffer solution (PBS; 0.1 M) was prepared by dissolving 0.1molNaCl and 0.1 mol Na_2HPO_4in 1L of doubly distilled water and adjusting the pH values by using 6mol L^{-1}aqueous HCl or 1 mol L^{-1}NaOH solution. For all electrochemical experiments, a Princeton Electrochemical Analyzer was used. The electrochemical cells consisted of three electrodes; a 2 mm diameter GCE, as working electrode, a platinum wire as the counter electrode and a saturated calomel electrode (SCE) as the reference electrode.

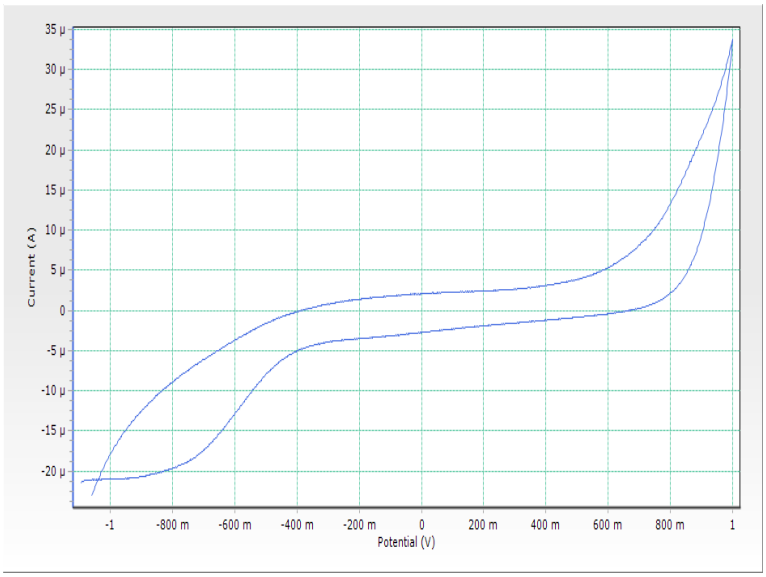

Fig. 9 Cyclic voltammogram of $[Co(HEDTA)N_3]^-$ complex

Table. 3 Result of CV spectrum

Range	Ep_a	Ep_c	ΔEp	Ip_a	Ip_c	Scanrate
-1 to +1	-730	780	1510	-11	3	100

The cyclic voltammogram of $[Co(HEDTA)N_3]^-$glassy carbon electrodeis shown in Fig.9. It shows the CV curves at different scan rates inthe domains of the anodic and cathodic processes. Anodic andcathodic scans are plotted on the same graph. Theelectrochemical reversibility of the anodic (I_a) andcathodic (I_c) processes has been carefully evaluated fromthe CV curves obtained at different scan rates. As it can be seen in fig. these processes are reversible. In a reversible process, the following Randles-Sevcik formula has being used:

$$i_{pa} = 2.69 \times 10^5 n^{3/2} AC_0 D_0^{½} \nu^{1/2}$$

where,

i_{pa} refers to the anodic peak current

n is the electron transfer number

A is the microscopic surface area of the electrode (cm^2),

D_0 is the diffusion coefficient ($cm^2\ s^{-1}$),

C_0 is the bulk concentration of cobalt azide(mol cm^{-3}) and

ν is the scan rate (Vs^{-1}).

3.5 Intercalative study of $[Co(HEDTA)N_3]^-$ complex with BSA

Absorption Spectroscopy Measurements

A solutionof 2.5 ml, containing appropriate concentration of BSA ($1x10^{-3}$ M), was titrated by successive additions of a 10 µl stock solution of $[Co(HEDTA)N_3]^-$ complex. Titrations were manually done by using micro pipette for the addition of complex.

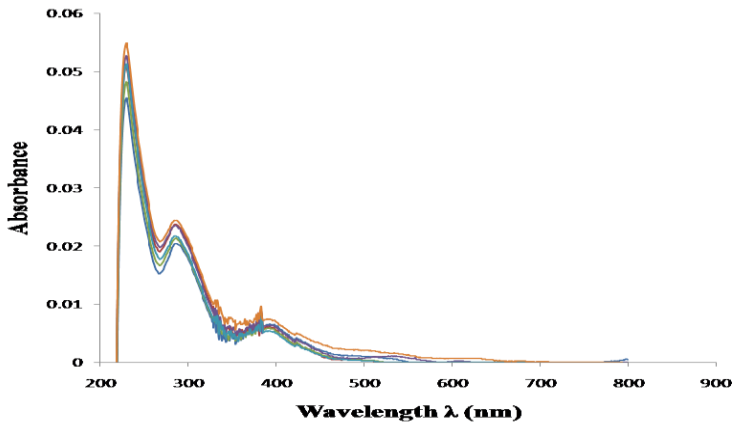

Fig. 10 Absorption spectra data of BSA ($1x10^{-3}$ M) in the presence of $[Co(HEDTA)N_3]^-$ ($0\text{-}5\times10^{-5}$ M)

Table.4 Absorption spectral data of BSA ($1x10^{-3}$M) in the presence of $[Co(HEDTA)N_3]^-$ ($0–5 \times 10^{-5}$ M)

[Complex]	λ_{max} (nm)	A
0	293	0.0201
1	290	0.0231
2	290	0.0207
3	290	0.0229
4	290	0.021
5	290	0.0238

Fig.10 shows the absorption spectrum of BSA in phosphate buffer (pH 8) containing $[Co(HEDTA)N_3]^-$ complex at different concentrations. In the presence of $[Co(HEDTA)N_3]^-$ complex the absorbance of BSA is increased markedly, without change in the location of the peak (280 nm). This inference is due to, while adding $[Co(HEDTA)N_3]^-$ complex to the solution of BSA some of the BSA molecules gets adsorbed on the surface of $[Co(HEDTA)N_3]^-$ complexand involved in the formation of ground state complex of the type [BSA . . . complex]. The newly formed complex also having absorption at 290 nm. This is the reason for increase in absorbance of BSA with the addition of $[Co(HEDTA)N_3]^-$ complex as supported by similar observations on repetition.

Determination of Apparent Association Constant (K_{app}) of BSA with $[Co(HEDTA)N_3]^-$ complex

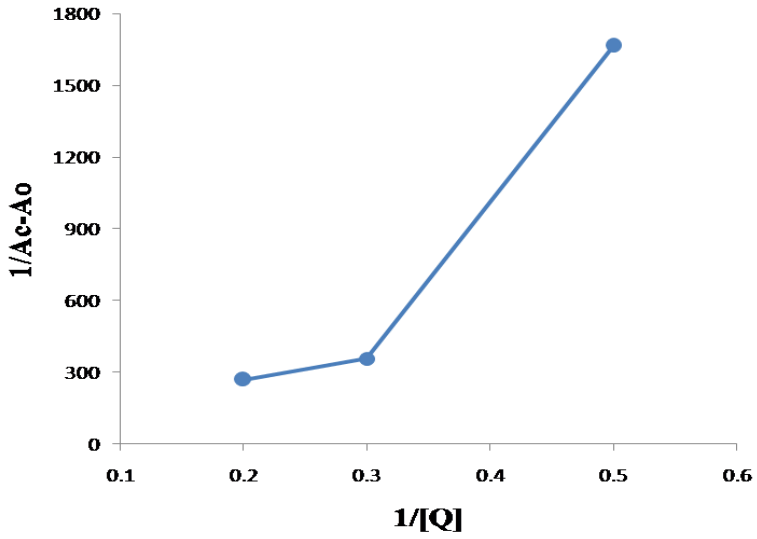

Fig. 11 Plot of 1/ (A_{obs} – A_0) Vs. 1/[Q]

The value of apparent association constant K_{app} was determined from this plot and it is found to be **$2.0x\ 10^4 M^{-1}$.**

3.5. a Intercalative studies of $[Co(HEDTA)N_3]^-$ complex with BSA

The increase in absorption of BSA while adding complex is due to the reaction between the quencher and BSA during the addition of quencher solution to BSA solution. The BSA molecules gets adsorbed on the surface of the complex and all involved in the formation of ground state complex (BSA-$[Co(HEDTA)N_3]^-$ complex). The newly formed complex also having the absorption at 280nm. This increase in absorption may be attributed to the formation of new complex.

The equilibrium for the formation of complex between BSA and $[Co(HEDTA)N_3]^-$ and complex is given by the following equation.

BSA+ $[Co(HEDTA)N_3]^- \rightarrow$ BSA…….. $[Co(HEDTA)N_3]^-$

According to Benesel and Hildebrand equation, K_{app} (apparent binding constant) is obtained[15].

K_{app}= [BSA…….$[Co(HEDTA)N_3]^-$/ [BSA] $[Co(HEDTA)N_3]^-$

A_{obs} = (1-α) C_0€$_{BSA}$ l+α C_0€$_c$l…….. (1)

Where A_{obs} absorbance is the observed absorbance of the solution containing different concentration of $[Co(HEDTA)N_3]^-$complex. (α)is the degree of association between BSA and$[Co(HEDTA)N_3]^-$complex. €$_{BSA}$and€$_c$ are the molar extinctions at the defined wavelength (lambda=280nm) for BSA and the formed complex respectively. C_o is the initial concentration of BSA and l is the optical path length.

Equation (1) can be expressed as equation 2 where A_0 and A_c are the absorbance of BSA and the complex at 280nm respectively with the concentration of C_0

A_{obs} = (1-α)A_0+αA_C.....(2)

At relatively high concentration of the quencher (α) can be replaced and the equation can be changed as follows.

$$\frac{1}{A_{obs} - A_o} = \frac{1}{A_c - A_o} + \frac{1}{K_{app}[A_c - A_o][Q]}$$

[Q] = $[Co(HEDTA)N_3]^-$

Based on the enhancement of absorption of surface complex, a linear relationship between $1/A_{obs}$-A_0 and the reciprocal concentration of the quencher with a slope equal to $1/K_{app}[A_C$-$A_0]$ and an intercept equal to $1/[A_c$-$A_0]$ was obtained.

3.5. b Intercalative study of $[Co(HEDTA)N_3]^-$ complex with DNA

Absorption Spectroscopy Measurements

The DNA binding experiments were performed at 30.0 ± 0.2°C. The DNA concentration per nucleotide was determined by electronic absorption spectroscopy using the known molar extinction coefficient value of 6600 M^{-1} cm^{-1} at 260 nm. 2.5 ml of solution, containing appropriate concentration of DNA ($1x10^{-5}$ M), was titrated by successive additions of a 10 µl stock solution of $[Co(HEDTA)N_3]^-$ complex respectively. Titrations were manually done by using micro pipette for the addition of complex. UV–visible spectra of all the solutions were recorded in the range of 200–800 nm.

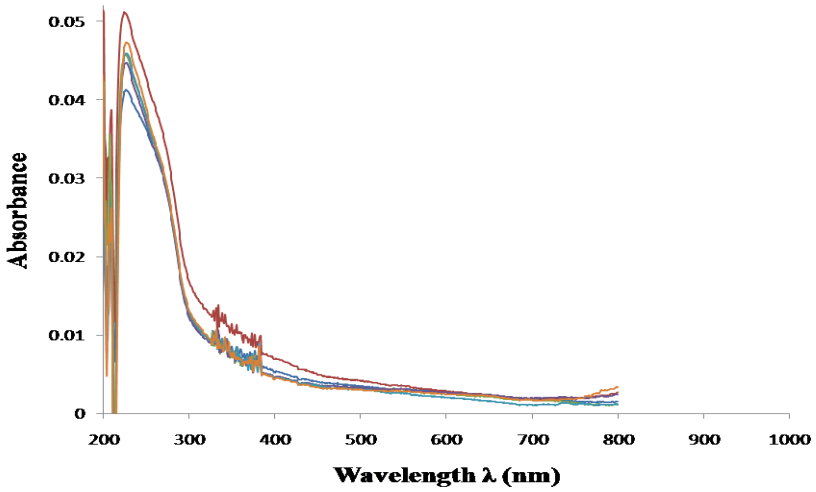

Fig. 12 Absorption spectra of DNA ($1x10^{-4}$ M) in the presence of $[Co(HEDTA)N_3]^-$ complex(0–5 x 10^{-5} M).

Table. 5 Absorption spectral data of DNA ($1x10^{-4}$ M) in the presence of $[Co(HEDTA)N_3]^-$ complex (0–5 x 10^{-5} M).

[Complex]	λ_{max} (nm)	A
0	235	0.0396
1	233	0.0488
2	233	0.0438
3	233	0.0430
4	233	0.0443
5	233	0.0458

Fig. 12 shows the UV absorption spectra of CT-DNA in the absence and presence of $[Co(HEDTA)N_3]^-$ complex. In the ultraviolet region from 200 to 300 nm, the complex had strong absorption peak at 233 nm. This spectra illustrates the influence of $[Co(HEDTA)N_3]^-$ complex onbinding modes of DNA. These data shows that increasing complex concentrationof $[Co(HEDTA)N_3]^-$leads to marked hyperchromicity and minorred shift of the Sored band of $[Co(HEDTA)N_3]^-$ complex. These strong spectral modifications suggestthat the complex interact with DNA by a combination of outside binding and intercalation.

Determination of Apparent Association Constant (K_{app}) of DNA with $[Co(HEDTA)N_3$ complex

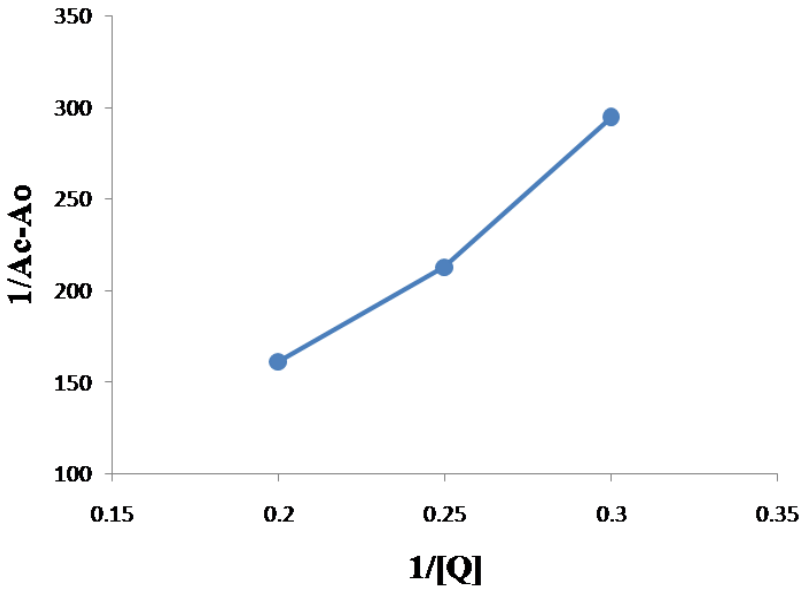

Fig. 13 Plot of 1/ (A_{obs} - A_0) Vs. 1/ Q

The value of apparent association constant K_{app} was determined from this plot and it is found to be **$0.7x\ 10^3\ M^{-1}$**.

3.5. c. Intercalative study of $[Co(HEDTA)N_3]^-$ complex with DNA

The increase in absorption of DNA while adding the complex is due to the reaction between the quencher (DNA) and $[Co(HEDTA)N_3]^-$ complex during the addition of quencher solution to $[Co(HEDTA)N_3]^-$ complex solution. The DNA molecules gets adsorbed on the surface of the complex and all involved in the formation of ground state complex (DNA-$[Co(HEDTA)N_3]^-$). The newly formed complex also having the absorption at 280nm. The increase in absorption may be attributed to the formation of new complex.

The equilibrium for the formation of complex between DNA and $[Co(HEDTA)N_3]^-$-Complex is given by the following equation.[17]

BSA+$[Co(HEDTA)N_3]^-$→ DNA…….. $[Co(HEDTA)N_3]^-$

K_{app}= [DNA……$[Co(HEDTA)N_3]^-$/ [DNA] $[Co(HEDTA)N_3]^-$

According to Benesel and Hildebrand equation K_{app} (apparent binding constant) is obtained.

A_{obs} = (1-α) $C_0€_{DNA}$ l + α $C_0€_c$l…….. (1)

Where A_{obs} absorbance is the observed absorbance of the solution containing different concentration of $[Co(HEDTA)N_3]^-$ complex.α is the degree of association between DNA and $[Co(HEDTA)N_3]^-$complex $€_{DNA}€_c$ are the molar extinction at the defined wavelength (lambda=279nm) for DNA and the formed complex respectively. C_o is the initial concentration of DNA and l is the optical path length. Equation (1) can be expressed as equation 2 where A_0 and A_c are the absorbance of DNA and the complex at 280nm respectively with the concentration of C_0

A_{obs} = (1-α)A_0+αA_C ……(2)

At relatively high concentration of the quencher (α) can be replaced and the equation can be changed as follows

$$\frac{1}{A_c - A_o} = \frac{1}{A_c - A_o} + \frac{1}{K_{app}[A_c - A_o][Q]}$$

[Q] = $[Co(HEDTA)N_3]^-$

Based on the enhancement of absorption of surface complex, a linear relationship between $1/A_{obs}$-A_0 and the reciprocal concentration of the quencher with a slope equal to $1/K_{app}[A_C$-$A_0]$ and an intercept equal to $1/[A_c$-$A_0]$ was obtained.

3.6 Intercalative study of $[Co(HEDTA)N_3]^-$ complex with BSA

Fluorescence Measurements

Binding studies of $[Co(HEDTA)N_3]^-$ complex was carried out with the most abundant protein BSA. Fig.14 shows the emission spectrum of BSA in water containing $[Co(HEDTA)N_3]^-$ complex at different concentration. In addition of the quencher, the absorption of BSA is increased markedly without change in location of the peak at 280nm.

Table. 6 Fluorescence spectral data of BSA ($1x10^{-3}$ M) in the presence of $[Co(HEDTA)N_3]^-$ complex (0–5 x 10^{-5} M)

[Complex]	λ_{max} (nm)	Fluorescence intensity
0	568	800
1	568	560
2	568	640
3	568	660
4	568	840
5	568	900

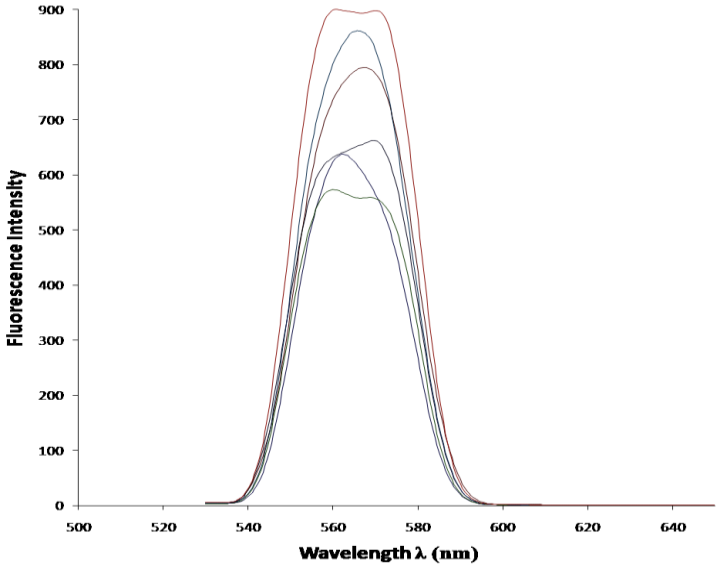

Fig. 14 Fluorescence spectra of BSA ($1x10^{-3}$ M) in the presence of the $[Co(HEDTA)N_3]^-$ complex(0–5 x 10^{-5} M).

Concentration [Q]	Fluorescence intensity	Io/I
0	800	-
1	560	1.4285
2	640	1.2500
4	840	0.9523
5	900	0.8888

3.6.1 Fluorescence quenching of BSA-$[Co(HEDTA)N_3]^-$ complex

Fig.14 shows the effect of increasing concentration of $[Co(HEDTA)N_3]^-$ complex on the fluorescence emission spectrum of BSA. Addition of $[Co[HEDTA]N_3]^-$ complex to the solution of BSA resulted in the quenching of its fluorescence emission.

The fluorescence quenching is described by Stern-Volmer relation.

$I_0/I = 1+K_{sv}[Q]=1+K_q\tau_0[Q]$----------(3)

Where Io and I are the emission intensities of BSA in the absence and presence of $[Co[HEDTA]N_3]^-$-complex. K_{sv} is the Stern-Volmer Constant. It is related to the bimolecular quenching rate constant (K_q) and $K_{sv}=K_q\tau_0$ where τ_0 is the average life time of BSA in the excited state which is 10^{-8} and [Q] is the concentration of the quencher. Accordingly to the equation (3) a linear plot is obtained when I_0/I is plotted against [Q] and it is showed in fig 15. The quenching rate constant is determined and it is found to be **$K_q=0.1377 \times 10^8 M^{-1}s^{-1}$.**

Table. 7 Determination of Quenching Constant (K_q) of BSA with [Co (HEDTA) N_3]$^-$ complex

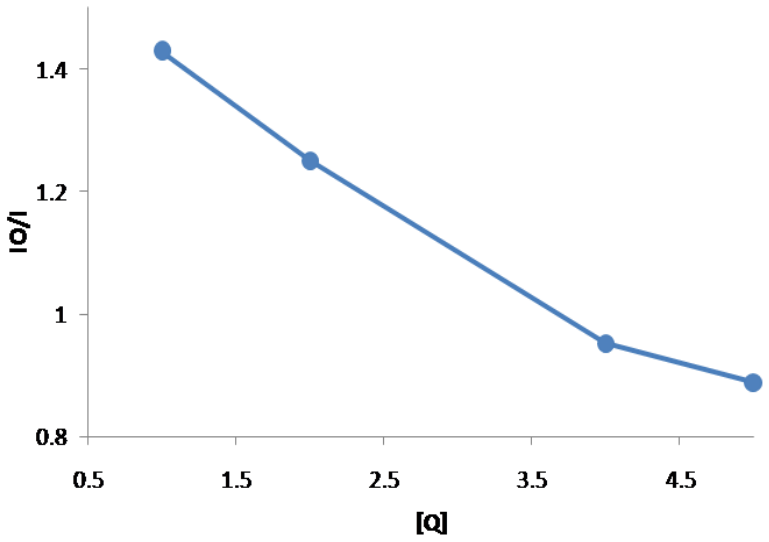

Fig.15 Plot of Io/IVs[Q]

5.6.2 Binding constant and number of binding sites

In general the quenching constant K_q of various kinds of quenchers to biopolymer is $2.0x10^{10}$. But for BSA-$[Co(HEDTA)N_3]^-$ complex system was found to be a higher and it is found to be$K_q=0.1377\times10^8$. This shows that the quenching of BSA by$[Co(HEDTA)N_3]^-$Complex is not dynamic in nature. Therefore it depends on the formation of complex between [Co $(HEDTA)N_3]^-$complex and BSA. For static quenching we can deduce the binding constant (K) because static quenching arises from the formation of complex between fluorophore and the quencher. Hence the binding constant was calculated by the following method.

The relationship between fluorescence intensity and the quencher medium can be deduced from the following equation.

$nQ+B \rightarrow Q_n$……..B

Where B is the fluorophore, Q is the quencher. nQ+B is the postulated complex between a fluorophore and n molecules of the quencher. The binding constant is given by the equation.

$K=[Q_n\ldots\ldots\ldots\ldots\ldots B]/[Q]^n[B]$

If the overall amount of bio molecule is B_0 then $[B_0]=[Q_n\ldots\ldots B]$

Where [B] is the concentration of unbound biomolecule.

$\log[F_0\text{-}F/F]=\log K+n\log[Q]$

Where K is the binding constant of $[Co\ (HEDTA)N_3]^-$-complex with BSA which can be determined from the intercept of the plot which is $\log[F_0\text{-}F]/F]$ V_s $\log[Q]$

Where F_0=fluorescence intensity in the absence of quencher

F=fluorescence intensity in the presence of quencher.

The calculated value of binding constant **$K=0.7909\ M^{-1}$** and the number of binding sites **n= 0.8540,** indicates the existence of number of binding sites.

Table. 8 Determination of Binding Constant (K) of BSA with $[Co(HEDTA)N_3]^-$ complex

$[Q]\ x\ 10^{-5}$	log [Q]	F	$F^0\text{-}F$	$\log (F^0\text{-}F/F)$
0	-	800	-	-
1	5.0	560	240	0.3679
2	4.698	640	160	0.6020
5	4.301	900	60	1.1760

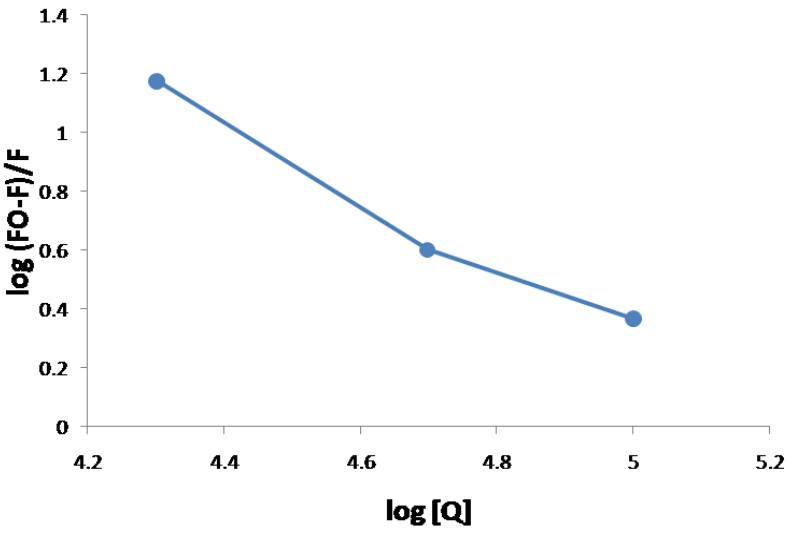

Fig. 16 Plot of $\log(F^o\text{-}F)/F$ Vs. log[Q]

5.6.3 Intercalative study of [Co (HEDTA)N_3]$^-$ complexes with DNA

Fluorescence Measurements

As the present cobalt (III) complex is non-emissive, ethidium bromide(EB) binding study was undertaken to gain support for the extent of binding of the complex with DNA. Ethidium bromide (EB) was shown to emit intense fluorescence light in the presence of DNA, due to its strong intercalation between the adjacent DNA base pairs. It was previously reported that the fluorescent light could be quenched by the addition of a second molecule.[11] The quenching extent of the fluorescence of EB binding to DNA is used to determine the extent of binding between the second molecule and DNA.

The competitive binding studies of [Co (HEDTA) N_3] $^-$ were carried out in Tris – HCl buffer (pH 7.2) by keeping EB - DNA solution containing [EB] = 2 µl and [DNA] = 8µl as constant and varying the concentration of complex. Fluorescence intensities at 610 nm (excited at 510 nm) were measured after each addition of complex.

In competitive ethidium bromide (EB) binding studies, the complexes [Co (HEDTA)N_3]$^-$ were added to DNA pretreated with EB ([EB] = 2µl, [DNA] = 8µl) and then emission intensities of DNA-induced EB were measured (Fig.18). Addition of a complex would quench the EB emission by either replacing DNA-bound EB (if it binds to DNA more strongly than EB) and/or by accepting the excited state electron from EB. The non-replacement based quenching has been suggested with DNA-mediated electron transfer from the excited ethidium bromide to acceptor metal complexes. As there is no complete quenching of the EB-induced emission intensity, an intercalative mode of DNA-binding of [Co(HEDTA)N_3]$^-$ observed values is ruled out. These values are lower than the classical intercalates which suggested that the complex [Co(HEDTA)N_3]$^-$ may be bind to DNA grooves. Stern – Volmer quenching constant K_{sv} of the complexes [Co(HEDTA)N_3]$^-$ to CT-DNA were determined from the equation Io/I = 1 + Ksvr where Io and I are fluorescence intensities of EB-DNA in absence and presence complex, respectively. K_{sv} is a linear Stern – Volmer quenching constant and r is the ratio of the total concentration of complex to that of DNA, [M]/[DNA]. In the linear fit plot of I_0/I *vs*[complex]/[DNA], K_{sv} is given by the ratio of slope to intercept. The apparent binding constant (K_{app}) was calculated from the equation K_{EB}[EB]/K_{app}[complex] where $\mathbf{K_{EB} = 1 \times 10^7}$, [EB] = 2 µl, and [complex] is the concentrations of the complex at 50% reduction of the emission intensity.

Table. 9 Fluorescence spectral data of DNA ($1x10^{-3}$ M) in the presence of [Co (HEDTA)N_3]$^-$ complex (0–5 x 10^{-5} M)

[Complex]	λ_{max} (nm)	Fluorescence Intensity
0	620	380
1	620	620
2	620	400
3	620	420
4	620	560
5	620	610

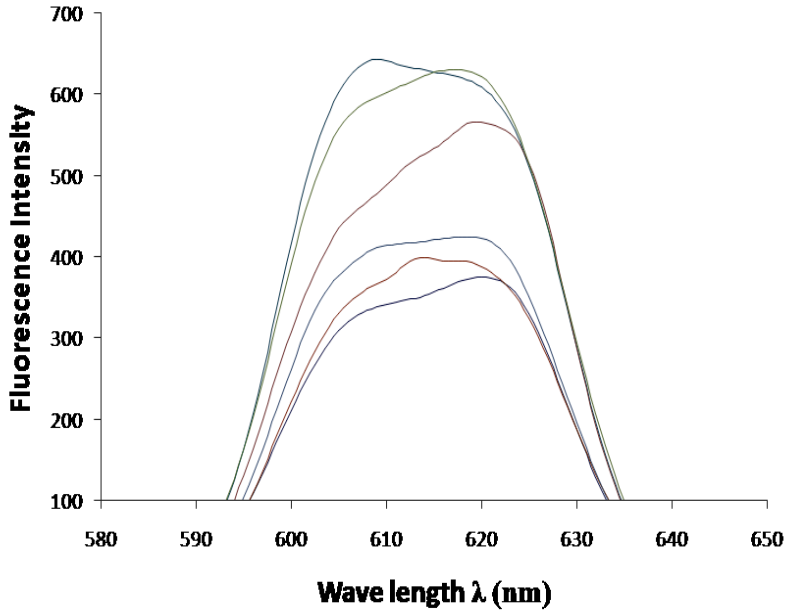

Fig. 17 Fluorescence spectra of DNA(1×10^{-4} M) in the presence of [Co(HEDTA)N_3]$^-$ complex (0-5×10^{-5}M)

Table. 10 Determination of Quenching Constant (K_q) of DNA with [Co(HEDTA)N_3]$^-$ complex

Concentration [Q]	Fluorescence intensity	Io/I
0	380	-
1	620	-
2	400	1.5500
4	560	1.1071
5	610	1.0163

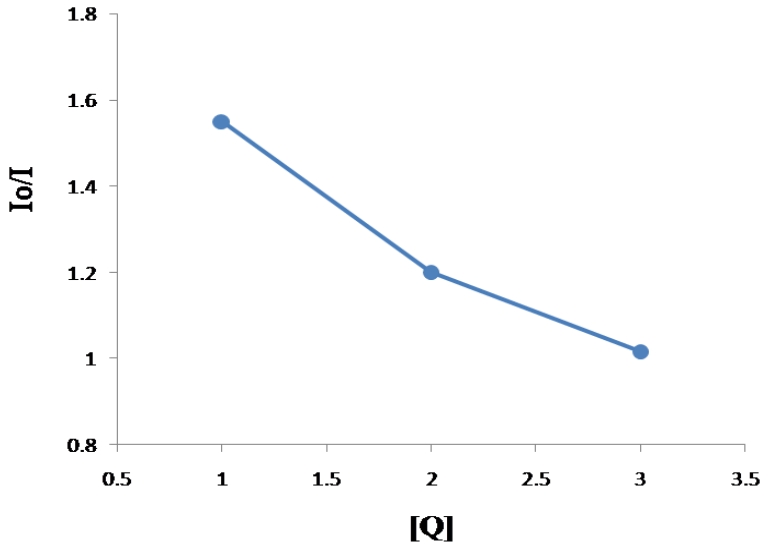

Fig. 18 Plot of Io/IVs[Q]

Table. 11 Determination of Binding Constant (K) of DNA with $[Co(HEDTA)N_3]^-$ complex

[Q] x 10^{-5}	log [Q]	F	F^0-F	log (F^0-F/F)
0	-	320	-	-
1	5.0	620		-
2	4.698	400	220	0.4499
4	4.397	560	60	1.0742
5	4.301	610	10	1.7923

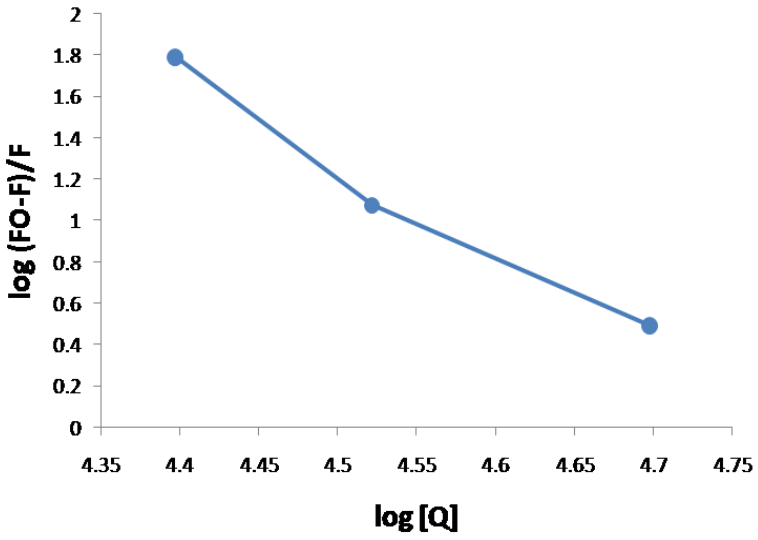

Fig. 19 Plot of log(F^o-F)/F Vs. log [Q]

5.6.3.a Binding constant and number of binding sites

In general the quenching constant K_q of various kinds of quenchers to biopolymer is 2.0×10^{-10}. But for BSA-$[Co(HEDTA)N_3]^-$ complex system was found to be a higher and it is found to be 0.1774×10^8. This shows that the quenching of DNA by Co-Complex is not dynamic in nature. Therefore it depends on the formation of complex between $[Co(HEDTA)N_3]^-$complex and DNA. For static quenching we can deduce the binding constant (K) because static quenching arises from the formation of complex between fluorophore and the quencher. Hence the binding constant was calculated by the following method.

The relationship between fluorescence intensity and the quencher medium can be deduced from the following equation.

$nQ+B \rightarrow Q_n$……..B

Where B is the fluorophore, Q is the quencher. nQ+B is the postulated complex between a fluorophore and n molecules of the quencher. The binding constant is given by the equation.

$K=[Q_n$……B$]/[Q]^n[B]$

If the overall amount of bio molecule is B_0 then $[B_0]=[Q_n$……B$]$

Where [B] is the concentration of unbound biomolecule.

$\log[F_0-F/F]=\log K+n\log[Q]$

Where K is the binding constant of $[Co\ (HEDTA)\ N_3]^-$complex with DNA which can be determined from the intercept of the plot which is $\log[F_0-F]/F]$versus log[Q]

Where F_0=fluorescence intensity in the absence of quencher

F=fluorescence intensity in the presence of quencher.

The calculated value of binding constant **K=1.3104 M^{-1}** and the number of binding sites **n= 0.2349**, indicates the existence of number of binding sites.

CONCLUSION

In the present work $[Co(HEDTA)N_3]^-$ complex has been synthesized by simple chemical method and characterized using Infrared spectral analysis, UV-Visible spectral analysis and Cyclic voltammetry. The interaction between $[Co(HEDTA)N_3]^-$ with BSA and CT-DNA has been studied by UV–visible and Fluorescence spectral analysis. The results presented clearly indicates that the $[Co(HEDTA)N_3]^-$ complex enhances the absorption of BSA and DNA

through complex formation. Binding studies of $[Co(HEDTA)N_3]^-$ complex has been investigated with the protein BSA and CT-DNA by UV-Visible spectrometry measurements and the apparent binding constants were determined. Experimental data reveals that the emission profiles of EB in the absence and presence of CT-DNA. EB does not emit fluorescence, but its emission intensity in the presence of DNA is greatly enhanced, due to its not strong intercalation between the adjacent DNA base pairs. Binding studies of $[Co(HEDTA)N_3]^-$ complex has been investigated with the protein BSA and CT-DNA by fluorescence spectral measurement. The binding constant were determined and it is found to be Binding constant K= 0.7909 M^{-1}, quenching constant $K_q=0.2278\times10^8$ $M^{-1}S^{-1}$ and number of binding sites n=0.8540.(BSA) and Binding constant K=1.3104 M^{-1}, quenching constant $K_q=0.2424\times10^8$ $M^{-1}S^{-1}$and number of binding sites n=0.2349(DNA).

ACKNOWLEDGEMENT

The authors are thankful to the management of Bishop Heber College for their kind support to do this work.

REFERENCE

1. Goswami, Tridib K., et al. "Ferrocene-conjugated copper (II) complexes of L-methionine and phenanthroline bases: Synthesis, structure, and photocytotoxic activity." *Organometallics*, 31.8 (2012): 3010-3021.
2. Kate, Anup N., et al. "Monitoring cellular uptake and cytotoxicity of copper (ii) complex using a fluorescent anthracene thiosemicarbazone ligand."*Bioconjugate chemistry*, 2013; 25.1: 102-114.
3. Nfor, Emmanuel N., et al. "A Novel Mixed Ligand Dinuclear Complex of Cobalt (II): Synthesis, Characterization and Magnetic Studies." *Crystal Structure Theory and Applications*, 2014; (2014).
4. Nfor, Emmanuel N., et al. "A Novel Mixed Ligand Dinuclear Complex of Cobalt (II): Synthesis, Characterization and Magnetic Studies." *Crystal Structure Theory and Applications*, 2014; (2014).
5. Lahiri, Debojyoti, et al. "Anaerobic DNA cleavage activity in red light and photocytotoxicity of (pyridine-2-thiol) cobalt (III) complexes of phenanthroline bases." *Dalton Transactions*, 2010; 39.7: 1807-1816.
6. Rajalakshmi, Subramaniyam, Manikantan Syamala Kiran and Balachandran Unni Nair. "DNA condensation by copper (II) complexes and their anti-proliferative effect on

cancerous and normal fibroblast cells." *European journal of medicinal chemistry*, 2014; 80: 393-406.

7. Rajalakshmi, Subramaniyam, Manikantan Syamala Kiran and Balachandran Unni Nair. "DNA condensation by copper (II) complexes and their anti-proliferative effect on cancerous and normal fibroblast cells." *European journal of medicinal chemistry*, 2014; 80: 393-406.
8. Thamilarasan, Vijayan, Arumugam Jayamani and Nallathambi Sengottuvelan. "Synthesis, molecular structure, biological properties and molecular docking studies on Mn II, Co II and Zn II complexes containing bipyridine–azide ligands." *European journal of medicinal chemistry*, 2015; 89: 266-278.
9. Rajendiran, Venugopal, et al. "Mixed-ligand copper (II)-phenolate complexes: effect of coligand on enhanced DNA and protein binding, DNA cleavage, and anticancer activity." *Inorganic chemistry*, 2007; 46.20: 8208-8221.
10. Gerald, Onyedika, Arinze Judith and Ogwuegbu Martin. "Studies on Extraction Behaviour of Cobalt (II) with Nitrobenzoylprazolone-5." (2013).
11. Gerald, Onyedika, Arinze Judith and Ogwuegbu Martin. "Studies on Extraction Behaviour of Cobalt (II) with Nitrobenzoylprazolone-5." (2013).
12. Kassab, M. M., S. U. El-Kameesy and M. M. Eissa. "A Study of Neutron and Gamma-Ray Interaction Properties with Cobalt-Free Highly Chromium Maraging Steel." *Journal of Modern Physics*, 2015; 6.11: 1526.
13. Moradi, Zohreh, Mozhgan Khorasani-Motlagh and Meissam Noroozifar. "Synthesis and biological evaluation of a new dysprosium (III) complex containing 2, 9-dimethyl 1, 10-phenanthroline." *Journal of Biomolecular Structure and Dynamics* just-accepted, 2015; 1-37.
14. Eshkourfu, Rabia, et al. "Synthesis, characterization, cytotoxic activity and DNA binding properties of the novel dinuclear cobalt (III) complex with the condensation product of 2-acetylpyridine and malonic acid dihydrazide." *Journal of inorganic biochemistry*, 2011; 105.9: 1196-1203.
15. Yang, Wen, et al. "Synthesis, structures and antibacterial activities of benzoylthiourea derivatives and their complexes with cobalt." *Journal of inorganic biochemistry*, 2012; 116: 97-105.
16. Lalia-Kantouri, Maria, et al. "Effect of cobalt (II) complexes with dipyridylamine and salicylaldehydes on cultured tumor and non-tumor cells: synthesis, crystal structure

investigations and biological activity." *Journal of inorganic biochemistry*, 2012; 117: 25-34.

17. Li, Jun-Ling, et al. "Bio-relevant cobalt (II) complexes with compartmental polyquinoline ligand: Synthesis, crystal structures and biological activities." *Journal of inorganic biochemistry*, 2015; 145: 19-29.
18. Pires, Bianca M., et al. "Azido-and chlorido-cobalt complex as carrier-prototypes for antitumoral prodrugs." *Journal of inorganic biochemistry*, 2016; 157: 104-113.
19. Jia, Lei, et al. "Synthesis, characterization, and antitumor activity of three ternary dinuclear copper (II) complexes with a reduced Schiff base ligand and diimine coligands in vitro and in vivo." *Journal of inorganic biochemistry*, 2016; 159: 107-119.
20. Tsiliou, Sofia, et al. "Cobalt (II) complexes with non-steroidal anti-inflammatory drug tolfenamic acid: Structure and biological evaluation." *European journal of medicinal chemistry*, 2012; 48: 132-142.
21. Arjmand, Farukh and Mohd Muddassir. "Design and synthesis of heterobimetallic topoisomerase I and II inhibitor complexes: In vitro DNA binding, interaction with 5′-GMP and 5′-TMP and cleavage studies." *Journal of Photochemistry and Photobiology B: Biology*, 2010; 101.1: 37-46.
22. Liang, Shu-Xuan, et al. "Experimental studies on the chemiluminescence reaction mechanism of carbonate/bicarbonate and hydrogen peroxide in the presence of cobalt (II)." *The Journal of Physical Chemistry A.*, 2008; 112.4: 618-623.
23. Arthi, P., et al. "Dinuclear manganese (II) complexes of hexaazamacrocycles bearing N-benzoylated pendant separated by aromatic spacers: Antibacterial, DNA interaction, cytotoxic and molecular docking studies." *Journal of Photochemistry and Photobiology B: Biology*., 2015; 153: 247-260.
24. Hiroshi, Sakiyama, et al. "Magnetic analyses of isosceles tricobalt (II) complexes containing two types of octahedral high-spin cobalt (II) ions." *Open Journal of Inorganic Chemistry*, 2011; (2011).
25. Bader Belhaj, Ali, et al. "Synthesis, structural and spectroscopic characterization of the bis (nitrito-N) octaethylporphyrin cobalt (III) complex." *Open Journal of Inorganic Chemistry* 2011; (2011).
26. Belghith, Yassin, et al. "Spectroscopic and molecular structure characterization of the bis (2-aminophenol) (5, 10, 15, 20-tetraphenylporphyrinato) cobalt (II) complex." *Open Journal of Inorganic Chemistry*, 2012; 2.04: 81.

27. Louie, A. Y. and T. J. Meade. "A cobalt complex that selectively disrupts the structure and function of zinc fingers." *Proceedings of the National Academy of Sciences*, 1998; 95.12: 6663-6668.
28. Beck, Wolfgang. "Metal complexes of biologically important ligands, CLXXII [1]. metal ions and metal complexes as protective groups of amino acids and peptides–reactions at coordinated amino acids." *Zeitschrift für Naturforschung B*, 2009; 64.11-12: 1221-1245.